PHYSICS AND CHEMISTRY OF SOLID STATE
V. 27, No. 1 (2026) pp. 158-164
Section: Physics

DOI: 10.15330/pcss.27.1.158-164

Vasyl Stefanyk Carpathian National University

ФІЗИКА І ХІМІЯ ТВЕРДОГО ТІЛА
Т. 27, № 1 (2026) С. 158-164
Фізико-математичні науки

PACS: 61.66.–f, 73.21.Ac, 73.21.Fg

ISSN 1729-4428 (Print)
ISSN 2309-8589 (Online)

B.A. Lukiyanets, D.V. Matulka

Qualitative analysis of differences in the physical properties of few-layer quasi-2D crystals

Lviv Polytechnic National University, Lviv, Ukraine; dariya.v.matulka@lpnu.ua

Quasi-2D crystals (graphite, layered crystals A_3B_6, transition metal, etc.) have a variety of unique properties that can vary widely by external factors, intercalation, etc. This explains the interest in such crystals both from the point of view of fundamental research and from that of practical use. The technological possibilities of obtaining few-layer fragments of quasi-2D crystals have become another way to achieve properties not inherent in bulk materials. This article presents a generalized model of few-layer fragments, which qualitatively highlights the factors responsible for the differences between bulk quasi-2D samples and their few-layer counterparts. The model's conclusions are in qualitative agreement with experimental and theoretical findings reported by other authors. This study also addresses the impact of external factors on the physical properties of samples with varying layer thicknesses.

Keywords: quasi-2D crystals; energy band gap; electronic spectrum; intercalation.

Received 18 November 2025; Accepted 09 February 2026; Published 27 March 2026.

Introduction

There are over five hundred crystals in nature that can be classified as quasi-2D. Although not strictly two-dimensional, they share several characteristics with true 2D materials. In 2004, Geim and Novoselov obtained a crystal that is truly two-dimensional – graphene [1], a single carbon layer exfoliated from graphite. Initial studies revealed its exceptional electrical and thermal conductivity and highlighted the potential for numerous applications [2–4]. Notably, graphene, being atomically thin, possesses a maximum specific surface area of approximately 2630 m^2/g, whereas analogous materials exhibit only about 100–1000 m^2/g. Consequently, this material is regarded as a promising candidate for application in high-capacity energy storage devices and supercapacitors.

Graphene's lack of a band gap gives it an exceptionally wide transmission region with a reflectance below 0.1%, while it absorbs only about 2.3% of white light, making it a highly transparent material. This property, coupled with the high carrier mobility exhibited by graphene, renders the material particularly suitable for solar cell applications. On the other hand, the lack of a band gap in graphene means there is a very low density of states in it. This creates problems for its use in devices that require electron flow control.

A further issue pertains to the occurrence of defects during the mechanical or chemical exfoliation of graphene. This process has been observed to diminish the electrical conductivity of the material, etc. To circumvent these and other problems, and to achieve a deeper understanding of graphene's nature, studies of structures consisting of few-layer graphene exfoliated from graphite become popular [5].

Significant changes in physical characteristics depending on its amount in structures were established. It is well established that the band structure of graphene can be described by an equation analogous to the relativistic Dirac equation. The resulting spectrum, known as the Dirac dispersion law, is distinguished by the absence of a band gap at the K points of the first Brillouin zone [6]. These points are known as Dirac points, where the conduction and valence bands collide. Two important features of the Dirac dispersion law are its linearity and the fact that the effective mass of carriers is zero. It has

been established that in bilayer graphene the dispersion relation becomes nonlinear, leading to the emergence of a band gap and a non-zero effective carrier mass. The physical properties of crystals with different layer numbers differ significantly. For example, this behavior contrasts with that of monolayer and bilayer graphene: the effective mass of carriers increases with increasing thickness, and trilayer graphene exhibits lower mobility than both monolayer and bilayer graphene.

Evidently, the remarkable properties of few-layer graphite have precipitated a resurgence of interest in few-layer quasi-2D crystals, which exhibit notable similarities to graphite. We demonstrate this correspondence using quasi-2D crystals as an example; these materials have been the focus of intensive scientific research and practical applications in spintronics, nanoelectronics, optoelectronics, and energy-storage devices [7]. They can be attributed to three large classes: graphite, layered crystals containing chalcogen (S, Se, Te), in particular crystals of the A_3B_6 type, and transition metal chalcogenides (TMDs) such as Ti, Zr, Hf, Ta, V, Nb, Cr, W, Mo, Pd, Pt. The representatives – MoS_2 (TMD), GaSe (A_3B_6), and graphite – are shown in Fig. 1.

All of them can be regarded as stacks ("sandwiches") of monoatomic planes—S–Mo–S, Se–Ga–Ga–Se, and a carbon plane, respectively. In the case of these sandwiches, the interatomic bonding is covalent or partially ionic-covalent, whereas adjacent sandwiches are held together by much weaker van der Waals forces. The distinct nature of atomic interactions along different crystallographic directions gives rise to strongly anisotropic physical properties of the crystals. This property is the underlying rationale for their classification as quasi-2D crystals.

The first report on the synthesis of TMDs appeared in the mid-1980s [8], while monocrystalline MoS_2 samples comprising several layers had been reported even earlier [9]. Lithium intercalation of MoS_2 enables the exfoliation of single or few layers from bulk MoS_2 [10]. This process is analogous to the production of graphene via exfoliation from graphite. Early studies of few-layer quasi-2D crystals revealed that exfoliated MoS_2 possesses properties substantially different from those of its bulk analogue [11,12]. Whereas bulk MoS_2 behaves as an indirect-band-gap semiconductor with negligible photoluminescence, exfoliated layers exhibit a direct band gap and a luminescence quantum efficiency exceeding that of the bulk by more than four orders of magnitude.

Significant differences in the bandgap width have been observed in other studies, depending on the number of layers in the samples, in both TMD [13], and A_3B_6 [14]. This is similar to what was previously found in multilayer grapheme [1].

Given the different component composition or arrangement of sandwiches (for example, in polytypes) in different quasi-2D crystals, the qualitative results of their studies will be different. However, an obligatory feature of any quasi-2D crystal is the existence of weakly interconnected energetically stable sandwiches. Given this feature, it is possible to create a generalized model if an arbitrary quasi-2D crystal at a qualitative level. It cannot claim to describe the quantitative characteristics of specific quasi-2D crystals, but it is capable of describing, in particular, characteristic changes in the spectrum of states during the transition from an arbitrary bulk quasi-2D crystal to its fragments.

I. Model and Calculations

Any quasi-2D crystal is actually three-dimensional. If it has orthogonal symmetry, then its $U(x,y,z)$ potential can be represented as: $(x,y,z) = U(x) + U(y,z)$. Then the stationary Schrödinger equation

$$(-\frac{\hbar^2}{2m}\nabla^2_{xyz} + U(x,y,z))\Psi(x,y,z) = E\Psi(x,y,z) \qquad (1)$$

is split into two independent differential equations:

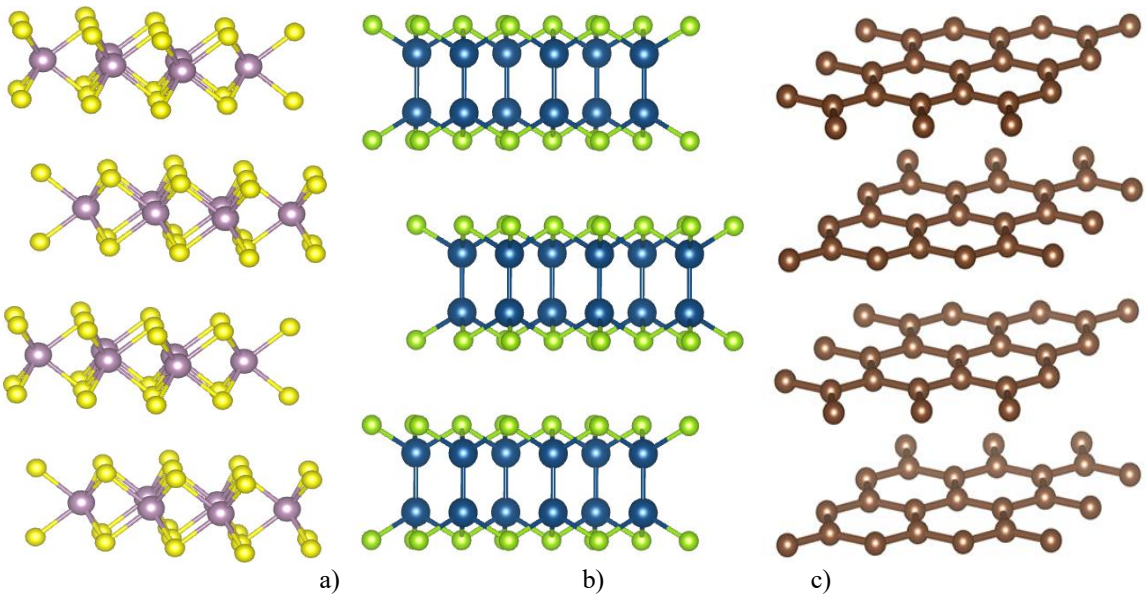

a) b) c)

Fig. 1. Crystal structures (side view) TDM MoS_2-type (yellow – S, violet– Mo) (a), β-GaSe (green– Se, blue – Ga) (b), graphite (brown circles – C) (c).

$$(-\frac{\hbar^2}{2m}\nabla_{yz}^2 + U(y,z))\phi(y,z) = E_1\phi(y,z) \qquad (2)$$

and

$$(-\frac{\hbar^2}{2m}\nabla_x^2 + U(x))\psi(x) = E_2\psi(x) \qquad (3)$$

In eq. (2) $\phi(y,z)$ is the Bloch wave function, which describes the energy state $E_1 = E(k_y,k_z) = \frac{\hbar^2(k_y^2+k_z^2)}{2m^*}$ in the case of an isotropic crystal in the ZOY plane (m^* is the effective mass of the electron).

Eq. (3) is used to study the electronic states in the mono- and bilayers whose potentials are shown in Figures 2(a) and 2(b), respectively. The model is represented as a sequence of wells and barriers (sandwiches), each corresponding to a specific region of the potential. In this framework, U_0 denotes the sandwich potential, while a and b represent the widths of the well and of the sandwich, respectively. For the monolayer, the positions are defined as $x_1 = \frac{a}{2}$ and $x_2 = \frac{a}{2} + b$. In the bilayer case, the positions are given by $x_1 = \frac{b}{2}$, $x_2 = \frac{b}{2} + a$, and $x_3 = a + \frac{3}{2}b$. This simplified representation allows for a clear analysis of the electronic states in both mono- and bilayer structures. The potential is assumed to be $U(x) \to \infty$ for $|x| \geq x_2$ in a mono-layer configuration and for $|x| \geq x_3$ in a bi-layer configuration.

The proposed models are fragments of the Kronig-Penney potential, which is used to describe the electronic structure of quantum wells and superstructures based on the envelope function approximation [15]. The simplified Kronig-Penney model has a wide range of applications. For example, it has been successfully used to study MQW structures of materials in the lighting industry and in solar cells (see, for example, [16]). Such theoretical models provide a qualitative understanding of electronic behavior and are in agreement with experimental data.

The choice of model along the normal to the layers (the c-axis) is determined by its relation to dimensional quantisation, which plays an important role in the physics of quasi-2D crystals.

In equation (3) wave functions in the i-th ranges with constant potentials being [17].

$$\psi_i(x) = a_i \exp(k_i x) + b_i \exp(-k_i x) \qquad (4)$$

Here k_i are the roots of the characteristic equation (3). They are given by $\sqrt{\frac{2m}{\hbar^2}(U_0 - E)}$ in the sandwich range and $\sqrt{\frac{2m}{\hbar^2}E}$. The index $i = 1$ is the range $x \in [0, x_1]$, while i= 2 corresponds to the ranges $x \in [x_1, x_2]$ and $x \in [x_2, x_3]$; see Figure 2(a) and (b).

The solutions Equation (1) in both the monolayer and the bilayer are symmetric, $\psi_i(x) = \psi_i(-x)$, and asymmetric, $\psi_i(x) = -\psi_i(-x)$. Stitching wave functions and their first derivatives at points where the potential creates a system of linear equations. A non-trivial solution is possible if the determinant, whose entries are the coefficients in a_i and b_i is equal to zero. The energy states, as will be shown below, are discrete states E_i. Thus, the spectrum of a quasi-2D crystal $E = E_i + \frac{\hbar^2(k_y^2+k_z^2)}{2m^*}$ is a set of sub-bands, i.e. discrete states E_i loaded with 2D zones of the layer plane.

In the case of quasi-2D semiconductors the potential for holes should be added to the potential for electrons of the conduction band. In general, such potentials are different. Below we have chosen such a potential as a mirror-symmetric to the potential of the electron of the conduction band. Then in a semiconductor there are two zones, each of which is a set of identical sub-bands separated by a forbidden band E_g.

Within the framework of a qualitative analysis, the choice of a mirror-symmetric potential and not affect the final conclusions of the work.

II. Results and Discussion

Let us consider equation (3). Its solutions will be determined by the initial points for the sub-bands. With parameters a = 0.8 nm, b = 0.8 nm and U_0= 5 eV, we obtain symmetric and antisymmetric solutions for the monolayer (Figure 3a) and for the bilayer (Figure 3b). Here the vertical lines pointing upwards correspond to symmetric states, while those pointing downwards correspond to states, while those pointing downwards correspond to antisymmetric states.

Figure 3 demonstrates that:

1. The density of states in the bilayer is higher than in the monolayer.

2. The ground state of the bilayer is closer to the band bottom (0.06 eV) than the ground state of the monolayer (0.40 eV).

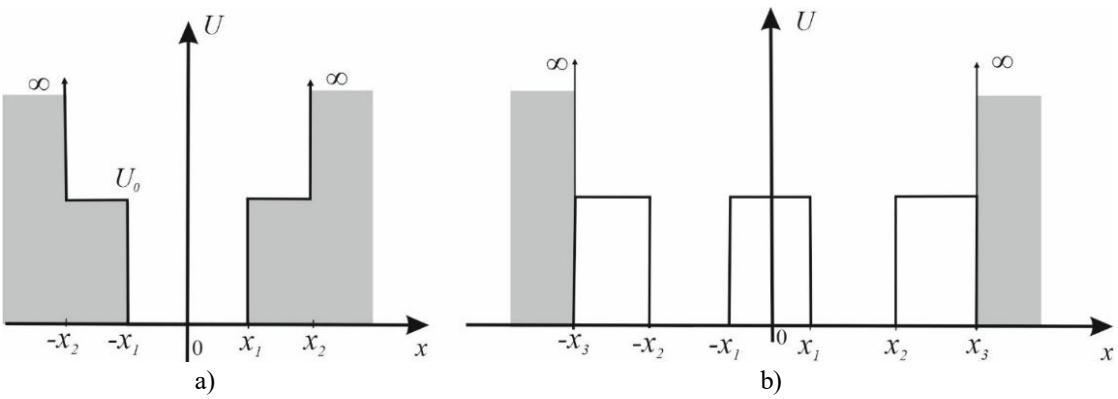

a) b)

Fig. 2. Potential along the c-axis of the monolayer (a) and bilayer (b).

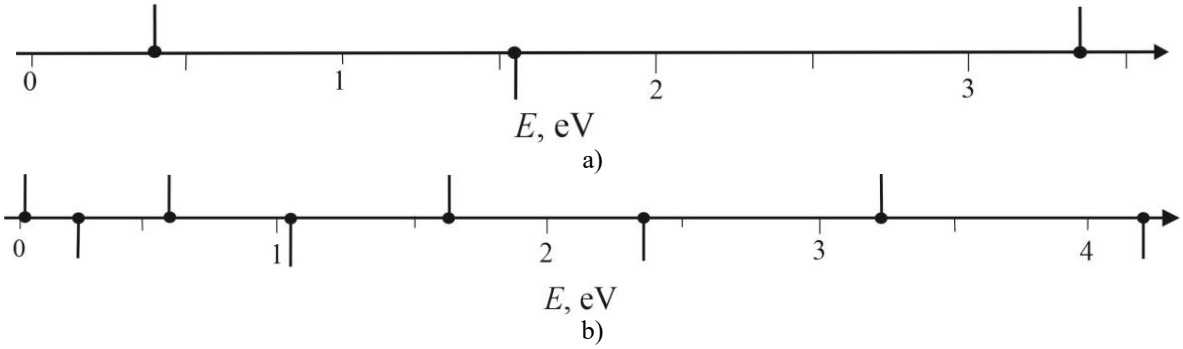

Fig. 3. Energy sub-barrier states of symmetric/asymmetric solutions of monolayer (a) and bilayer (b).

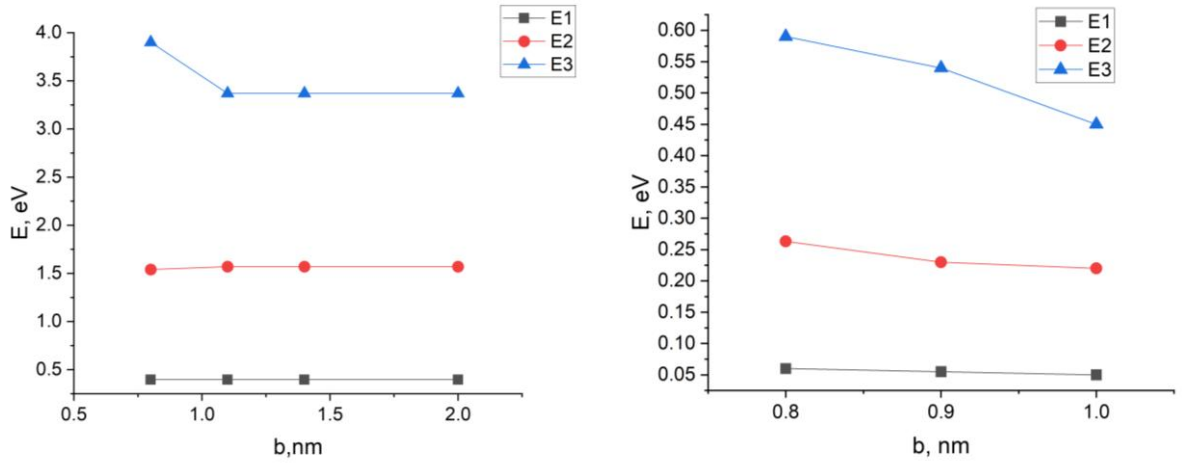

a) b)

Fig. 4. Dependence of the position of the three lowest states on barrier width b for a monolayer (left) and a bilayer (right) structures (b) dependence on the well width a at fixed U_0 = 5 eV and barrier width b = 0.8 nm.

3. The obtained results for a quasi-2D semiconductor with mirror-symmetric potentials allow us to establish such an important characteristic as the optical band gap. It is known that such a width is an energy gap that determines the minimum energy of a photon capable of transferring an electron from the ceiling of the valence band to the lowest state of the conduction band at $\frac{\hbar_2(k_y^2+k_z^2)}{2m^*} = 0$. If the origin of the conduction band is chosen at the origin of coordinates, then the positions of discrete hole states, identical to the positions of electrons shifted by $-E_g$.

Then in the mono-layer taking into account the selection rules, the transition can occur between the highest symmetrical level of the valence band $-(E_g + 0.40)$ eV and the lowest asymmetrical level in the conduction band of 1.54 eV, i.e. the optical band gap $E_g + 1.94$ eV. In the bi-layer a similar transition between the symmetrical state of the valence band $-(E_g + 0.06)$ eV and the lowest asymmetrical state of the conduction band of 0.26 eV, i.e. optical band gap is $+(E_g + 0.32)$ eV.

Thus, in both cases, the optical band gap is larger than in the bulk crystal; however, in the monolayer, this value is much larger than that of the bilayer.

Changes in the electron spectrum upon the transition to a few layers are caused by quantum confinement effects due to dimensionality reduction. These changes are qualitatively consistent with a number of theoretical and experimental studies on specific few-layer quasi-2D crystals. In particular, noticeable consequences of such changes were observed in optical absorption GaSe via highly sensitive differential transmission measurement [18] or in optical absorption band-edge GaSe under strain [19]; in observation by first principles spectrum calculations MoS_2, a prototypical layered transition-metal dichalcogenide and related TmS_2 (Tm = W, Nb, Re) [20]; in density functional calculations layer-dependent bandgaps and the strain effect in InSe [21]; in the experimental study of the intensity of emitted light for GaSe samples or the Raman spectrum of few-layer InSe, GaSe [22] , etc.

Several studies have shown that the electronic properties of few-layer quasi-2D crystals undergo significant restructuring under mechanical deformation [19,21].

Let us analyze the dependence of the positions of the three lowest states on the sandwich potential and geometric parameters in two such cases:

(a) dependence on the barrier width b at fixed U_0 = 5 eV and well width a = 0.8 nm.

(b) dependence on the well width a at fixed U_0 = 5 eV and barrier width b = 0.8 nm,

Figures 4 and 5 show that the level positions depend monotonically on an increase in the width of the sandwiches and wells, with varying degrees of decrease. In the linear approximation, the angular coefficients when

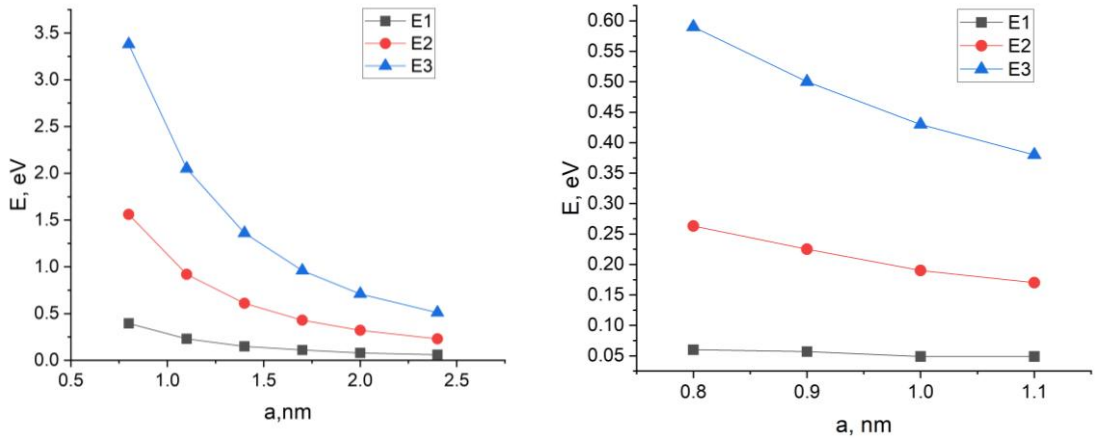

a) b)

Fig. 5. Dependence of the position of the three lowest states on the well width for a monolayer (a) and of a bilayer (b).

b = 0.8 nm and U_0=5 eV with variables a are presented in Table 1.

And in the case of a = 0.8 nm and U_0 = 5 eV and with variable sandwich width angular coefficients are presented in Table 2.

Table 1.
Linear approximation of the angular coefficients when b=0.8 nm and U_0=5 eV.

Mono- dE/da, eV/nm	- 0.21	- 0.8	- 1.7
Bi- dE/da, eV/nm	-0.03	- 0.3	-0.7

Table 2.
Linear approximation of the angular coefficients when a=0.8 nm and U_0=5 eV.

Mono- dE/db, eV/nm	0	0	0
Bi- dE/db, eV/nm	0	-0.18	-0.40

From comparing such tables, the following tendencies can be noted:

1. The states of both the monolayer and the bilayer change as the width of the well increases, but the change is significantly greater in the monolayer than in the bilayer.

2. With an increase in the width of sandwich b (for its real values), the states in the monolayer remain practically constant, whereas in the bilayer, a non-zero response is only observed for excited states and the ground state remains constant.

Thus, changing the well width is the most effective way to alter the properties of the mono- and bilayer. In the context of the ground state, the effect of the change is also evident in the bilayer, though to a significantly lesser extent than that observed in the monolayer.

There are significant differences in the behaviour of mono- and bi-layers under the same parameters. Moreover, these differences can be made even more pronounced by applying a number of factors. Among them:

– mechanical stresses [23, 24];
– hydrostatic or axial compression along the c-axis [23];
– intercalation [25];
– laser and ultrasound radiation [26].

The following two factors will be considered in greater detail: hydrostatic or axial compression, and intercalation.

The first factor is compression. The pressure-related behaviour of quasi-2D crystals can be illustrated by the results of work [23]. Based on high-pressure (0.30 GPa) X-ray diffraction measurements in TMD 3R-MoN_2 (an analogue of MoS_2), a significant difference was found between the axial compressibility along the a-axis and that along the c-axis. The lattice constant a_0=2.854Å at a pressure $p = 20.4$ GPa decreased to a = 2.776Å, i.e. $\frac{a_0}{a}$= 1.03, while the lattice constant along the c-axis decreased from c_0= 15.938Å to c = 14.380Å, i.e. $\frac{c_0}{c}$= 1.12. This shows that the quasi-two-dimensional crystals are much more compressible along the c-axis than in the layer plane. As a result of the specified pressure change, the cell volume changed from V_0=112.42Å^3 to V= 95.968Å^3. (Note, that the c-axis constant includes a van der Waals gap, which is absent in the a-axis constant.)

Given the sandwich's low compressibility, we can conclude that the narrowing of the van der Waals gap is the determining cause of the volume change. Let us present another argument in support of this statement. In graphite, the elastic constant (modulus) in the plane of the layers is $C_{11} = 106$ GPa, while the elastic constant along the c-axis is $C_{33} = 38.5$ GPa [27]. With this ratio of elastic moduli during compression, the volume will be determined almost exclusively by the change in the width of the van der Waals gap.

Given the extraordinary influence of the van der Waals gap width on quasi-2D crystal properties, another factor affecting this width should be mentioned: intercalation. This is the process of introducing or removing foreign atoms or molecules into the van der Waals gap, which results in a change in its width. These conclusions were drawn at the outset of intercalation studies reported in [28]. This work presents the results of searches for materials with high transition temperatures $T_c$to the superconducting state. To this end, 50 TMDs were intercalated with all possible inorganic and organic molecules. It was found that intercalation increases the

width of crystals along the c-axis. Sometimes, depending on the intercalate, such changes can be impressive. For example, when TaS_2 was intercalated with stearamides, the van der Waals gap increased from 6 Å to 57Å.

The above estimates are for quasi-2D crystals. For few-layer crystals, they may differ slightly, but not by enough to change the qualitative results.

Conclusions

Based on the proposed unified model of a quasi-2D crystal, the obtained results are qualitatively consistent with those of experimental and theoretical studies by other authors.

Calculations performed in the monolayer and bilayer structures show that the density of states in the bilayer is higher than in the monolayer, and the optical band gap in mono significantly exceeds that in the bilayer. The results of the studies also showed that changing the width of the well is the most effective way to change the properties of any mono- and bilayer structures.

The proposed model allows us to be confident that the conclusions and predictions of the model will remain valid for a qualitative understanding of physical phenomena in any quasi-two-dimensional crystals, and its results can be used to guide the design and development of layered structures with individual properties for specific technological applications.

Lukiyanets B.A. – Doctor of Physical and Mathematical Sciences, Professor of the Department of Applied Physics and Nanomaterials Science;
Matulka D.V. – Candidate of Technical Sciences, Associate Professor of the Department of Applied Physics and Nanomaterials Science.

[1] A. K. Geim, K. S. Novoselov, *The rise of graphene*, Nature Materials, 6, 183 (2007); https://doi.org/10.1038/nmat1849.
[2] P. Esquinazi, *Basic Physics of Functionalized Graphite*, Springer Series in Materials Science 244 (2016); https://doi.org/10.1007/978-3-319-39355-1.
[3] S. K. Tiwari, S. Sahoo, N. Wang, A. Huczko, *Graphene research and their outputs: Status and prospect*, Journal of Science: Advanced Materials and Devices, 5, 10 (2020); https://doi.org/10.1016/j.jsamd.2020.01.006.
[4] C. N. R. Rao, K. Gopalakrishnan, A. Govindaraj, *Synthesis, properties and applications of graphene doped with boron, nitrogen and other elements*, Nano Today, 324 (2014); https://doi.org/10.1016/j.nantod.2014.04.010.
[5] V. Kumar, A. Kumar, D.-J. Lee, S.-S. Park, *Estimation of Number of Graphene Layers Using Different Methods*, Materials, 14, 4590 (2021); https://doi.org/10.3390/ma14164590.
[6] G. W. Semenoff, *Condensed-matter simulation of a three-dimensional anomaly*, Phys. Rev. Lett., 53, 2449 (1984); https://doi.org/10.1103/PhysRevLett.53.2449.
[7] X. Duan, H. Zhang, *Introduction: Two-Dimensional Layered Transition Metal Dichalcogenides*, Chemical Reviews, 124, 10619 (2024); https://doi.org/10.1021/acs.chemrev.4c00586.
[8] P. Joensen, R. Frindt, S. R. Morrison, Single-layer MoS_2, *Mater.* Res. Bull., 21, 457 (1986); https://doi.org/10.1016/0025-5408(86)90011-5.
[9] R. Frindt, *Single crystals of MoS_2 several molecular layers thick*, J. Appl. Phys., 37, 1928– (1966); https://doi.org/10.1063/1.1708627.
[10] W. Zhou et al., *Intrinsic Structural Defects in Monolayer Molybdenum Disulfide*, Nano Letters, 13, 2615 (2013); https://doi.org/10.1021/nl4007479.
[11] A. Splendiani, L. Sun, Y. Zhang, T. Li, J. Kim, C.-Y. Chim, G. Gall, F. Wang, *Emerging Photoluminescence in Monolayer MoS_2,* Nano Letters, 15, 1271 (2010); https://doi.org/10.1021/nl903868w.
[12] K. F. Mak, C. Lee, J. Hone, J. Shan, T. F. Heinz, *Atomically Thin MoS_2: A new direct-gap semiconductor*, Phys. Rev. Lett., 105, 136805 (2010); https://doi.org/10.1103/PhysRevLett.105.136805.
[13] L. Zheng, X. Wang, H. Jiang, M. Xu, W. Huang, Z. Liu, *Recent progress of flexible electronics by 2D transition metal dichalcogenides*, Nano Research, 15, 2413 (2022); https://doi.org/10.1007/s12274-021-3779-z.
[14] C. Song, S. Huang, C. Wang, J. Luo, H. Yan, *The optical properties of few-layer InSe*, J. Appl. Phys., 128, 060901 (2020); https://doi.org/10.1063/5.0018480.
[15] J. Bastard, A. Brum, R. Ferreira, *Electronic states in semiconductor heterostructures*, Solid State Physics, 44, 230 (1991); https://doi.org/10.1016/S0081-1947(08)60092-2.
[16] Y. Zhang, Y. Wang, *Energy band analysis of MQW structures in the Kronig–Penney model*, J. Modern Physics, N4, 568 (2013); https://doi.org/10.4236/jmp.2013.47130.
[17] R. L. Liboff, Introductory Quantum Mechanics, 4th ed., Addison-Wesley, Boston (2003).
[18] A. Budweg, D. Yadav, A. Grupp et al., *Control of excitonic absorption by thickness variation in few-layer GaSe,* Phys. Rev. B, 100, 045404 (2019); https://doi.org/10.48550/arXiv.1712.06330.
[19] D. Maeso, S. Pakdel, H. Santos, N. Agraït, J. J. Palacios, E. Prada, G. Rubio-Bollinger, *Strong modulation of optical properties in rippled 2D GaSe via strain engineering,* Nanotechnology, 30 (2019); https://doi.org/10.1088/1361-6528/ab0bc1.
[20] A. Kuc, N. Zibouche, *Th. Heine, Influence of quantum confinement on the electronic structure of the transition metal sulfide TS_2,* Phys. Rev. B, 83, 245213 (2011); https://doi.org/10.1103/PhysRevB.83.245213.

[21] D. Andres-Penares, A. Cros, J. P. Martinez-Pastor, J. F. Sanchez-Royo, *Quantum size confinement in gallium selenide nanosheets: band gap tunability versus stability limitation,* Nanotechnology, 28 (2017); https://doi.org/10.1088/1361-6528/aa669e.
[22] M. Usman, S. Golovynskyi, D. Dong, Y. Lin, Z. Yue, M. Imran, B. Li, H. Wu, L. Wang, *Raman Scattering and Exciton Photoluminescence in Few-Layer GaSe: Thickness- and Temperature-Dependent Behaviors*, J. Phys. Chem. C, 126 (25), 10459 (2022); https://doi.org/10.1021/acs.jpcc.2c02127.
[23] X. Zhou, M. Yan, M. Dong, D. Ma, X. Yu, J. Zhang, Y. Zhao, S. Wang, *Phase stability and compressibility of 3R-MoN_2 at high pressure,* Scientific Reports, 9, 10524 (2019); https://doi.org/10.1038/s41598-019-46822.
[24] A. Segura, *Layered indium selenide under high pressure*, Crystals, 8, 206 (2018); https://doi.org/10.3390/cryst8050206.
[25] S.A. Safran, *Stage Ordering in Intercalation Compounds*, Solid State Physics, 40, 183 (1987); https://doi.org/10.1016/S0081-1947(08)60692-X.
[26] H. Wang, M. Xu, H. Ji, T. He, W. Li, L. Zheng, X. Wang, *Laser-assisted synthesis of two-dimensional transition metal dichalcogenides: a mini review*, Front. Chem., 11, 1195640 (2023); https://doi.org/10.3389/fchem.2023.1195640.
[27] A. Bosak, M. Krisch, M. Mohr, J. Maultzsch, C. Thomsen, *Elasticity of single-crystalline graphite: Inelastic X-ray scattering study*, Phys. Rev. B, 75, 153408 (2007); https://doi.org/10.1103/PhysRevB.75.153408.
[28] F. R. Gamble, J. H. Osiecki, M. Cais, R. Pisharody, F. J. DiSalvo, T. H. Geballe, *Intercalation Complexes of Lewis Bases and Layered Sulfides: A Large Class of New Superconductors*, Science, 174 (4008), 493–497 (1971); https://doi.org/10.1126/science.174.4008.493.

Б.А. Лукіянець, Д.В. Матулка

Якісний аналіз відмінностей у фізичних властивостях кількашарових квазі-2D кристалів

Національний університет «Львівська політехніка», Львів, Україна; dariya.v.matulka@lpnu.ua

Квазі-2D кристали (графіт, шаруваті кристали A_3B_6, перехідні метали тощо) мають низку унікальних властивостей, які можуть значно змінюватися під впливом зовнішніх факторів, інтеркаляції тощо. Це пояснює інтерес до таких кристалів як з точки зору фундаментальних досліджень, так і з точки зору практичного застосування. Технологічні можливості отримання кількашарових фрагментів квазі-2D кристалів стали ще одним способом досягнення властивостей, нехарактерних об'ємним матеріалам. У пропонованій роботі представлено узагальнену модель кількашарових фрагментів, яка якісно висвітлює фактори, що відповідають за відмінності між об'ємними квазі-2D зразками та їх кількашаровими аналогами. Висновки моделі якісно узгоджуються з експериментальними та теоретичними результатами, опублікованими іншими авторами. У роботі також розглядається вплив зовнішніх факторів на фізичні властивості зразків з різною товщиною шарів.

Ключові слова: квазі-2D кристали, енергетична щілина, електронний спектр, інтеркаляція.